

# X-Ray Evidence for Flare Density Variations and Continual Chromospheric Evaporation in Proxima Centauri

Manuel Güdel<sup>1</sup>, Marc Audard<sup>1,2</sup>, Stephen L. Skinner<sup>3</sup>, Matthias I. Horvath<sup>4</sup>

## ABSTRACT

Using the *XMM-Newton* X-ray observatory to monitor the nearest star to the Sun, Proxima Centauri, we recorded the weakest X-ray flares on a magnetically active star ever observed. Correlated X-ray and optical variability provide strong support for coronal energy and mass supply by a nearly continuous sequence of rapid explosive energy releases. Variable emission line fluxes were observed in the He-like triplets of O VII and Ne IX during a giant flare. They give direct X-ray evidence for density variations, implying densities between  $2 \times 10^{10} - 4 \times 10^{11} \text{ cm}^{-3}$  and providing estimates of the mass and the volume of the line-emitting plasma. We discuss the data in the context of the chromospheric evaporation scenario.

*Subject headings:* stars: activity — stars: coronae — stars: flare — stars: individual (Proxima Centauri) — X-rays: stars

## 1. Introduction

The identification of the physical mechanisms underlying the heating of coronae of magnetically active stars to some 10–100 Million degrees (MK) remains as one of the fundamental problems of high-energy stellar astrophysics. Among the non-steady heating mechanisms, explosive release of energy by flares has received considerable attention in solar physics (e.g., Porter et al. 1995; Krucker & Benz 1998; Parnell & Jupp 2000; Aschwanden et al. 2000),

---

<sup>1</sup>Paul Scherrer Institut, Würenlingen und Villigen, CH-5232 Villigen PSI, Switzerland

<sup>2</sup>Present address: Columbia Astrophysics Laboratory, Mail code 5247, Columbia University, 550 West 120th Street, New York, NY 10027, USA

<sup>3</sup>Center for Astrophysics and Space Astronomy, University of Colorado, Boulder CO, 80309-0389, USA

<sup>4</sup>Institute of Astronomy, ETH Zentrum, CH-8092 Zürich, Switzerland

in particular since the statistical ensemble of flares, if extrapolated to small “micro-” or “nano-” flares, may provide enough energy to explain the total coronal energy losses.

There is mounting evidence that flares also play a fundamental role in coronal heating of magnetically active stars. The quiescent X-ray luminosity  $L_X$  is correlated with the flare rate in X-rays (Audard et al. 2000) and in the optical (Doyle & Butler 1985; Skumanich 1985). Statistically, the hotter X-ray emitting plasma component is more variable than the cooler one, indicating that flares may be involved (Giampapa et al. 1996). Recent studies of the flare frequency in magnetically active stars as a function of the flare energy indicate power-law distributions that may be sufficient to explain all coronal radiative losses (Audard et al. 2000; Kashyap et al. 2002; Güdel et al. 2003).

The physical mechanisms that transport the hot plasma into the corona are, however, less clear. A favored model in solar physics predicts that an initial release of high-energy particles (detected by their radio or prompt optical emission, see below) deposits energy in the cool chromosphere, inducing an overpressure that drives hot material into the corona (“chromospheric evaporation”). As for any coronal heating mechanism, a large density increase is predicted which should be measurable in high-resolution X-ray spectra, in particular in density-sensitive He-like triplets of O VII and Ne IX.

We present novel observations of Proxima Centauri, the nearest star to the Sun (distance = 1.3 pc), with the *XMM-Newton* satellite, providing new important evidence for frequent chromospheric evaporation. Detailed models will be presented in a forthcoming paper.

## 2. Target and Observations

Proxima Centauri is a dM5.5e dwarf revealing considerable coronal activity. Its “quiescent” X-ray luminosity  $L_X \approx 5 - 10 \times 10^{26} \text{ erg s}^{-1}$  is similar to the Sun’s despite its  $\approx 50$  times smaller surface area. It has attracted the attention of most previous X-ray observatories (Haisch et al. 1980, 1981, 1983, 1990, 1995, 1998; Wargelin & Drake 2002).

*XMM-Newton* (Jansen et al. 2001) observed the star on 2001 August 12 during 65 ks of exposure time. For our light curve analysis, we used the most sensitive soft X-ray detector system presently available, namely the three combined European Photon Imaging Cameras (EPIC; Turner et al. 2001; Strüder et al. 2001) with a total effective area of  $\approx 2000 \text{ cm}^2$  at 1 keV and  $\approx 2500 \text{ cm}^2$  at 1.5 keV (with the medium filters inserted). The flares thus recorded are the weakest yet observed on an active star. To minimize CCD pile-up, the small window modes were used. Background light curves were extracted from CCD fields outside the source region. The Reflection Grating Spectrometers (RGS; den Herder et al.

2001) simultaneously recorded high-resolution X-ray spectra between 0.35–2.5 keV, with a resolving power of  $E/\Delta E \approx 300$  (FWHM) around the O VII lines at  $\approx 22$  Å. The Optical Monitor (OM; Mason et al. 2001) observed the star through its U band filter in high-time resolution mode. All data were analyzed using the *XMM-Newton* Science Analysis System (SAS versions 5.3 and 5.3.3).

Relevant extracts of the observations are shown in Figures 1 and 2. The first 45 ks of the observation reveal low-level emission around  $L_X = 6 \times 10^{26}$  erg s $^{-1}$  (0.15–10 keV). Thanks to the high sensitivity, much of the emission is resolved into a succession of weak X-ray flares (Figure 1). The smallest discernible events show  $L_{X,0.15-10} = 2 \times 10^{26}$  erg s $^{-1}$  and an integrated X-ray energy loss of  $E_{X,0.15-10} \approx 1.5 \times 10^{28}$  erg, corresponding to modest solar flares. Most importantly, many (although not all) of these flares are preceded by a short pulse in the optical U band (Figure 1). A large flare monitored almost in its entirety governed the final 20 ks of the observation, with a peak  $L_{X,0.15-10} \approx 3.7 \times 10^{28}$  erg s $^{-1}$  and  $E_{X,0.15-10} \approx 1.5 \times 10^{32}$  erg (Figure 2). Due to pile-up in the MOS detectors, we used only the PN data for the light curve analysis of this flare. Again, a large optical burst accompanies the X-ray flare during its increase. The figure also shows spectral extracts of the He-like triplets of O VII and Ne IX referring to different phases of the large flare. The line flux ratios are clearly variable, an aspect that will be discussed in detail below.

### 3. Results and Discussion

We now seek an interpretation within the evaporation scenario. During a flare, high-energy electrons are thought to be accelerated in the corona from where they travel toward the magnetic footpoints in the chromosphere. They induce a prompt signal in the optical U band (3000–4000 Å), probably owing to Balmer emission or blackbody radiation, or both (Hudson et al. 1992; Neidig & Kane 1993; Hawley et al. 1995). Their bulk kinetic energy heats the chromospheric gas to several MK, building up a pressure gradient that drives the hot plasma into the corona, thus increasing the coronal density and the soft X-ray emission. Since the optical signal  $L_O$  approximately traces the rate of energy deposited by the electrons (Hudson et al. 1992), and the X-ray losses  $L_X$  are a measure of the accumulated coronal thermal energy, the time integral of the optical signal should resemble the X-ray light curve,

$$L_X(t) \propto \int_0^t L_O(t') dt' \quad (1)$$

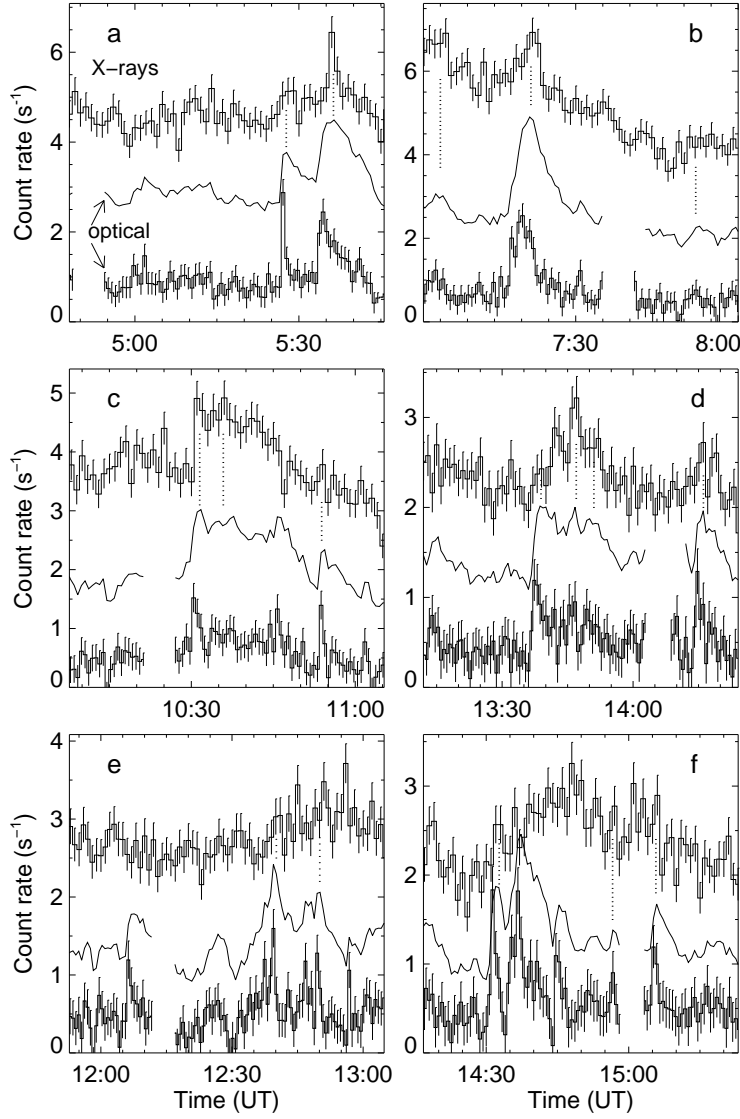


Fig. 1.— Time correlations between X-ray and optical flares. The upper curves in each panel show the co-added EPIC X-ray light curve (bin size 60 s, 0.15–4.5 keV). The lower curves illustrate the optical signal, binned to 40 s for optimum flare detection (and scaled in flux by a factor of 0.2 and shifted along the y-axis for illustration purposes; the time gaps are of instrumental origin). The thick solid line is a convolution of the optical light curve with a cut-off exponential function, and often closely resembles the X-ray signal (vertical dotted lines mark suggestive examples). Panels a and b: Correlated single flares. Panels c and d: Groups of flares. Panels e and f: Poor detailed correlation, but optical flare groups occur during general X-ray increases.

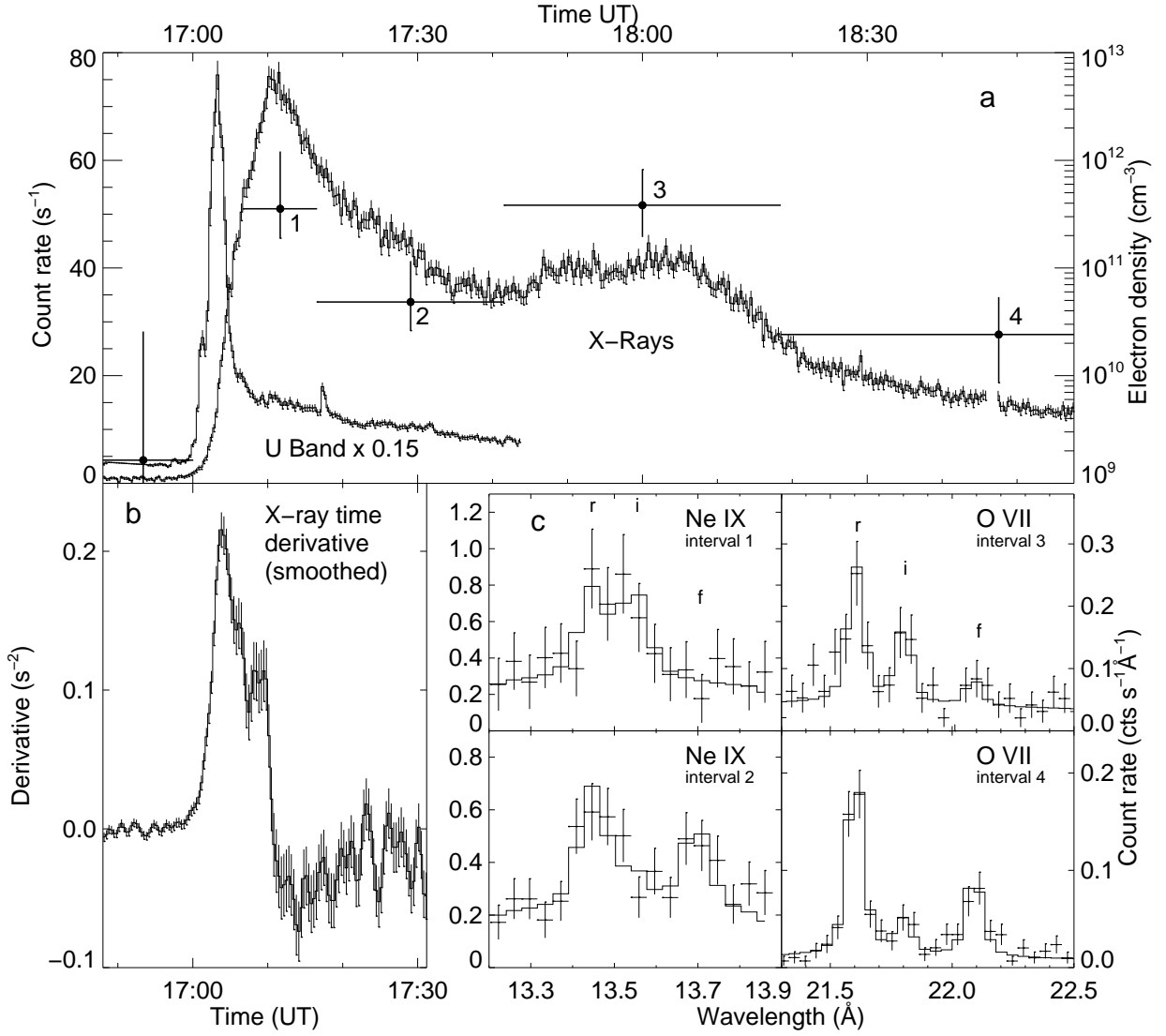


Fig. 2.— Large flare on Proxima Centauri. The upper panel (a) shows the EPIC PN X-ray (0.15–10 keV) and the preceding (scaled) optical light curves (bin size = 20 s). The crosses refer to the logarithmic axis on the right side and indicate the electron densities as measured from O VII lines. The arms in the vertical direction indicate the (linear)  $1\sigma$  error bars. Panel b is the smoothed time derivative of the X-ray light curve. It closely resembles the optical signal. Panels c illustrate He-like triplets with variable  $R$  ratios obtained during the four intervals marked in panel a, two examples for O VII and two for Ne IX. The histograms represent fits with three narrow lines each. (The O VII triplets of intervals 1 and 2 are very similar to those of intervals 3 and 4, respectively).

where the integration starts at a point in time preceding the flare ( $t' = 0$ ). In other words, the time derivative of the X-ray light curve should mimic the optical signal:

$$\frac{dL_X}{dt} \propto L_O. \quad (2)$$

Equation 1 is appropriate for testing faint signals, whereas equation 2 requires strong signals but is sensitive to details in the light curves. This important diagnostic has been observed in the solar corona, known as the Neupert Effect (using radio or hard X-ray emissions instead of U band radiation; Neupert 1968; Dennis & Zarro 1993), but has rarely been detected in stellar observations, especially in low-level emissions (Doyle et al. 1986, 1988), presumably owing to the limited sensitivity of previous X-ray devices. Qualitative evidence is seen in some strong flares (e.g., de Jager et al. 1986, 1989; Schmitt et al. 1993; Hawley et al. 1995). We suggest that each of our optical signals is the equivalent of an impulsive burst, while the associated X-ray flares are the signatures of the subsequent chromospheric evaporation. A surprising aspect is the high repetition rate of such processes in Proxima Centauri.

While hot plasma is accumulated in the corona, the X-ray emission of any plasma packet decays nearly exponentially due to cooling. Equation 1 in this form does not consider cooling; we therefore include a decay term by convolving the optical light curve with a cut-off exponential decay profile ( $e^{-t/\tau}$  for  $t \geq 0$  and zero for  $t < 0$ ). A decay time of  $\tau = 200$  s is found to be appropriate, and the convolution is shown by the thick solid curves in Figures 1a-f. After the convolution, a high level of correlation with the X-rays reveals itself in many coincident peaks and similar light curve shapes (Figures 1a,b). Suggestive examples are marked by vertical dotted lines. The optical light curve often predicts the subsequent X-ray behavior, revealing an intimate connection between the two emissions. The correlation holds even for some flare groups (Figures 1c,d). In some cases, the detailed correlation is poor although optical flare groups cluster during X-ray flux increases (Figures 1e,f). The large flare allowed us to compute its time derivative (Figure 2b). It traces the optical signal closely until after the optical flare peak, when uncorrelated cooling mechanisms take over. Here,  $\tau$  was not considered as it appears that ongoing heating on time scales longer than  $\tau$  dominates over cooling.

The X-ray flux  $F$  from a collisional plasma is proportional to the volume emission measure (EM),  $F = \text{const} \int n_e n_H dV \approx 0.84 \text{ const} \int n_e^2 dV$  where  $n_e$  is the electron density,  $n_H$  is the hydrogen (or proton) density, and  $dV$  is the source volume element; the proportionality constant is the line emissivity (Mewe et al. 1985). The determination of  $V$  and  $n_e$  from fluxes alone is therefore a degenerate problem. It can be circumvented by using the He-like spectral line triplets as a diagnostic for  $n_e$ . The relevant triplets of the O VII and Ne IX ions are each formed by radiative decays to the ground state, namely the resonance transition  $r$  ( $1s^2 \ ^1S_0 - 1s2p \ ^1P_1$ ), the intercombination transition  $i$  ( $1s^2 \ ^1S_0 - 1s2p \ ^3P_{1,2}$ ),

and the forbidden transition  $f$  ( $1s^2\ ^1S_0 - 1s2s\ ^3S_1$ ). In cool stars with negligible ultraviolet continuum radiation, the flux ratio  $R = f/i$  is sensitive to  $n_e$  because electron collisions can excite the  $^3S_1$  to the  $^3P$  state before the former decays radiatively (Gabriel & Jordan 1969; Porquet et al. 2001). The data reveal strong variations of  $R$  along the flare (examples in Figure 2c). The characteristic  $n_e$  derived from O VII reaches  $\approx 4 \times 10^{11}\text{ cm}^{-3}$  during the flux maxima, but is much lower ( $\approx 2 \times 10^{10}\text{ cm}^{-3}$ ) during the decays (crosses in Figure 2a). Previous attempts to estimate stellar coronal flare densities spectroscopically used lines in the extreme ultraviolet range, but density variations were difficult to constrain (e.g., Monsignori-Fossi et al. 1996; for a marginal X-ray result, see Stelzer et al. 2002). Qualitatively similar variations are seen in the Ne IX triplet (Figure 2c), although blends of the  $i$  line thwart a precise quantitative interpretation. The strongly variable  $f$  line alone suggests that plasma around 4–5 MK (the maximum formation temperature of Ne IX) attained densities across the density sensitivity range of this triplet,  $10^{11} - 2 \times 10^{12}\text{ cm}^{-3}$  (Porquet et al. 2001).

To derive the associated EM, we measured the total flux  $F_{\text{OVII}}$  of the O VII lines used above. We found that  $F_{\text{OVII}}$  is nearly proportional to the 0.15–10 keV EPIC count rate. This is important because O VII lines are efficiently formed only in a temperature range of  $1 \lesssim T \lesssim 4$  MK. We conclude that variations of the EM-weighted formation temperature of these lines are not the dominant factor for the variability of  $F_{\text{OVII}}$ . The ratio  $G = (f + i)/r$  provides an independent test since it is a temperature indicator for the O VII line-forming plasma (Gabriel & Jordan 1969; Porquet et al. 2001). We infer characteristic temperatures,  $T_G = 1.5\text{--}3.5$  MK, that cluster around the maximum formation temperature ( $T_{\text{OVII}} \approx 2$  MK) but do not show a clear correlation with  $F_{\text{OVII}}$ . We will therefore approximate the O VII emitting plasma as being isothermal at  $T_{\text{OVII}}$ ; systematic errors thus introduced for the EM are no larger than a factor of  $\approx 2$  (see tables in Mewe et al. 1985). For a homogeneous source at  $T_{\text{OVII}}$ ,  $F_{\text{OVII}} \propto n_e^2 V$ . Therefore,  $V \propto F_{\text{OVII}}/n_e^2$ , and the total mass  $M$  involved is  $M \propto F_{\text{OVII}}/n_e$ . We used emissivities from Mewe et al. (1985) referring to solar photospheric composition. From spectral fits in XSPEC (Arnaud 1996), we found an abundance of oxygen of  $0.52 \pm 0.08$  times the solar photospheric value (Anders & Grevesse 1989). For the primary peak, its decay, the secondary peak, and its decay, the masses of O VII emitting plasma thus amount to  $M \approx 4.8 \times 10^{14}\text{ g}$ ,  $2.1 \times 10^{15}\text{ g}$ ,  $3.2 \times 10^{14}\text{ g}$ , and  $2.5 \times 10^{15}\text{ g}$ , respectively, while  $V \approx 7.0 \times 10^{26}\text{ cm}^3$ ,  $2.3 \times 10^{28}\text{ cm}^3$ ,  $4.3 \times 10^{26}\text{ cm}^3$ , and  $5.3 \times 10^{28}\text{ cm}^3$ , respectively. The potential energy of a  $10^{15}\text{ g}$  plasma packet at a height of  $9 \times 10^3\text{ km}$  (the pressure scale height at  $2 \times 10^6\text{ K}$  for a radius of  $10^{10}\text{ cm}$  and a stellar mass of  $0.2M_\odot$ , see Haisch et al. 1983 and references therein) is  $2.5 \times 10^{29}\text{ erg}$ . This compares with the total thermal energy content of the same plasma,  $E \approx 1.65 \times (3/2)MkT/m_H \approx 4 \times 10^{29}\text{ erg}$ , while the total radiated X-ray energy from the cooler plasma component at 0.2 keV (determined from a spectral fit) is approximately  $1.7 \times 10^{31}\text{ erg}$  during the complete flare (using a peak EM

of  $1 \times 10^{50} \text{ cm}^{-3}$ , a decay time of 4300 s, and a cooling loss rate of  $4 \times 10^{-23} \text{ erg s}^{-1} \text{ cm}^3$ ), necessitating considerable replenishment of the cool material during the flare.

Even after consideration of the uncertainties due to variations of  $T_G$ , it is clear that densities, masses and volumes of the plasma accessible by O VII increase during the flare. Coronal density increases are a consequence of any heating mechanism in closed loops. It is the preceding optical impulsive emission that strongly supports chromospheric evaporation induced by electron beams. Solar white-light flares are closely correlated in time with hard X-ray bursts, suggesting that this phase relates to electron bombardment of the chromosphere (Hudson et al. 1992; Neidig & Kane 1993), while soft X-rays and higher densities are evolving more gradually. Since plasma cooling becomes important early in the flare development, the relatively cool O VII emitting plasma component is not only augmented due to heating of chromospheric material, but also due to cooling of hotter material that has initially reached temperatures beyond the formation range of O VII lines, hence the continuous increase of masses and volumes during the decay.

The low flux of the weaker flares and their strong mutual overlap prohibit individual density measurements, but integration of larger segments shows appreciable changes in  $R$  as well, with the highest-density episode related to the segment in Figure 1b (an increase of at most a factor of ten over the average). Furthermore, the time behavior of several optical and X-ray flares that expresses itself as a Neupert Effect is similar to the behavior seen in the large flare, indicating that the same processes repeat at a much higher cadence at lower energy levels such that they govern the X-ray emission most of the time. We do not find a one-to-one correspondence between all optical and X-ray flares, but this is no different on the Sun (Dennis & Zarro 1993). Some groups of small optical flares occur, however, during a general increase of the soft X-ray light curve.

The present observations suggest an important role of chromospheric evaporation in active stellar coronae. The resulting high plasma densities appear to be a critical element for the high X-ray luminosities of magnetically active stars.

Helpful comments by the referee are acknowledged. Research at PSI has been supported by the Swiss National Science Foundation (grant 2000-058827). The present project is based on observations obtained with *XMM-Newton*, an ESA science mission with instruments and contributions directly funded by ESA Member States and the USA (NASA).



## REFERENCES

- Anders, E., & Grevesse, N. 1989, *Geochim. Cosmochim. Acta*, 53, 197
- Arnaud, K. A. 1996, in *Astronomical Data Analysis Software and Systems V*, ed. G. Jacoby & J. Barnes (San Francisco: ASP), 17
- Aschwanden, M. J., Tarbell, T. D., Nightingale, R. W., Schrijver, C. J., Title, A., Kankelborg, C. C., Martens, P. C. H., & Warren, H. P. 2000, *ApJ*, 535, 1047
- Audard, M., Güdel, M., Drake, J. J., & Kashyap, V. L. 2000, *ApJ*, 541, 396
- de Jager, C., et al. 1986, *A&A*, 156, 95
- de Jager, C., et al. 1989, *A&A*, 211, 157
- den Herder, J. W., et al. 2001, *A&A*, 365, L7
- Dennis, B. R., & Zarro, D. M. 1993, *Solar Phys.*, 146, 177
- Doyle, J. G., & Butler, C. J. 1985, *Nature*, 313, 378
- Doyle, J. G., Butler, C. J., Byrne, P. B., & van den Oord, G. H. J. 1988, *A&A*, 193, 229
- Doyle, J. G., Butler, C. J., Haisch, B. M., & Rodonò, M. 1986, *MNRAS*, 223, 1P
- Gabriel, A. H., & Jordan, C. 1969, *MNRAS*, 145, 241
- Giampapa, M. S., Rosner, R., Kashyap, V., Fleming, T. A., Schmitt, J. H. M. M., & Bookbinder, J. A. 1996, *ApJ*, 463, 707
- Güdel, M., Audard, M., Kashyap, V. L., Drake, J. J., & Guinan, E. F. 2003, *ApJ*, in press
- Haisch, B. M., Antunes, A., & Schmitt, J. H. M. M. 1995, *Science*, 268, 1327
- Haisch, B.M., Butler, C.J., Foing, B., Rodonò, M., & Giampapa, M.S. 1990, *A&A*, 232, 387
- Haisch, B. M., Harnden, F. R. Jr., Seward, F. D., Vaiana, G. S., Linsky, J. L., & Rosner, R. 1980, *ApJ*, 242, L99
- Haisch, B. M., Kashyap, V., Drake, J. J., Freeman, P. 1998, *A&A*, 335, L101
- Haisch, B. M., Linsky, J. L., Bornmann, P. L., Stencel, R. E., Antiochos, S. K., Golub, L., & Vaiana, G. S. 1983, *ApJ*, 267, 280
- Haisch, B. M., et al. 1981, *ApJ*, 245, 1009

- Hawley, S. L., et al. 1995, *ApJ*, 453, 464
- Hudson, H. S., Acton, L. W., Hirayama, T., & Uchida, Y. 1992, *PASJ*, 44, L77
- Jansen, F., et al. 2001, *A&A*, 365, L1
- Kashyap, V. L., Drake, J. J., Güdel, M., & Audard, M. 2002, *ApJ*, in press
- Krucker, S., & Benz, A. O. 1998, *ApJ*, 501, L213.
- Mason, K., et al. 2001 *A&A*, 36, L36
- Mewe, R., Gronenschild, E. H. B. M., & van den Oord, G. H. J. 1985, *A&AS*, 62, 197
- Monsignori-Fossi, B. C., Landini, M., del Zanna, G., & Bowyer, S. 1996, *ApJ*, 466, 427
- Neidig, D. F., & Kane, S. R. 1993, *Solar Phys.*, 143, 201
- Neupert, W. M. 1968, *ApJ*, 153, L59
- Parnell, C. E., & Jupp, P. E. 2000, *ApJ*, 529, 554
- Porquet, D., Mewe, R., Dubau, J., Raassen, A. J. J., & Kaastra, J. S. 2001, *A&A*, 376, 1113
- Porter, J. G., Fontenla, J. M., & Simnett, G. M. 1995, *ApJ*, 438, 472
- Schmitt, J. H. M. M., Haisch, B., & Barwig, H. 1993, *ApJ*, 419, L81
- Skumanich, A. 1985, *Aust. J. Phys.*, 38, 971
- Stelzer, B., et al. 2002, *A&A*, 392, 585
- Strüder, L., et al. 2001, *A&A*, 365, L18
- Turner, M. J. L., et al. 2001, *A&A*, 365, L27
- Wargelin, B. J., & Drake, J. J. 2002, *ApJ*, 578, 503